

Surface mass balance of Davies Dome and Whisky Glacier on James Ross Island, north-eastern Antarctic Peninsula, based on different volume-mass conversion approaches

Zbyněk Engel^{1*}, Filip Hrbáček², Kamil Láska², Daniel Nývlt², Zdeněk Stachon²

¹Charles University, Faculty of Science, Department of Physical Geography and Geocology, Albertov 6, 128 43 Praha, Czech Republic

²Masaryk University, Faculty of Science, Department of Geography, Kotlářská 2, 611 37 Brno, Czech Republic

Abstract

This study presents surface mass balance of two small glaciers on James Ross Island calculated using constant and zonally-variable conversion factors. The density of 500 and 900 kg·m⁻³ adopted for snow in the accumulation area and ice in the ablation area, respectively, provides lower mass balance values that better fit to the glaciological records from glaciers on Vega Island and South Shetland Islands. The difference between the cumulative surface mass balance values based on constant (1.23 ± 0.44 m w.e.) and zonally-variable density (0.57 ± 0.67 m w.e.) is higher for Whisky Glacier where a total mass gain was observed over the period 2009–2015. The cumulative surface mass balance values are 0.46 ± 0.36 and 0.11 ± 0.37 m w.e. for Davies Dome, which experienced lower mass gain over the same period. The conversion approach does not affect much the spatial distribution of surface mass balance on glaciers, equilibrium line altitude and accumulation-area ratio. The pattern of the surface mass balance is almost identical in the ablation zone and very similar in the accumulation zone, where the constant conversion factor yields higher surface mass balance values. The equilibrium line altitude and accumulation-area ratio determined for the investigated glaciers differ by less than 2m and 0.01, respectively. The annual changes of equilibrium line altitude and the mean values determined over the period 2009–2015 for Whisky Glacier (311 ± 16 m a.s.l.) and Davies Dome (393 ± 18 m a.s.l.) coincide with the values reported from Bahía del Diablo Glacier on Vega Island but differ from the glaciological records on South Shetland Islands.

Key words: glacier mass balance, constant conversion, zonally-variable conversion, Antarctica

DOI: 10.5817/CPR2019-1-1

Received November 15, 2018, accepted March 27, 2019.

*Corresponding author: Z. Engel <engel@natur.cuni.cz>

Acknowledgements: The authors acknowledge funding from the Czech Science Foundation project (GC16-14122J). Fieldwork was supported by the crew of Mendel Station financed by the Ministry of Education, Youth and Sports of the Czech Republic (project no. LM2015078 and CZ.02.1.01/0.0/0.0/16_013/0001708). We thank Kristián Brat, Tomáš Franta, Tomáš Jagoš, Pavel Kapler, Jan Kavan, Pavel Ševčík, Martin Slezák, Peter Váczí, Vítězslav Vlček and Ondřej Zvěřina for research assistance in the field.

Introduction

Glaciers and ice caps (hereafter referred to as glaciers) cover 132,900 km² around the Antarctic Ice Sheet, representing 18% of the glacier area on Earth, excluding the ice sheets (Pfeffer *et al.* 2014). Despite the large extent of glaciers in the Antarctic and Subantarctic very few mass-balance records are available for this region. The surface mass balance records are important for understanding observed glaciers changes and their relationship to climate fluctuations in both local and regional scale. Therefore, *in situ* measurements represent one of the primary data source for glacier monitoring and projection of their future volumetric changes. In the Antarctic Peninsula (AP) region, glaciers with continuous mass-balance measurements spanning

more than 10 years include Bahía del Diablo Glacier on Vega Island, Hurd and Johnsons glaciers on Livingston Island (South Shetland Islands, SSI), Bellingshausen Ice Dome on King George Island (SSI) and Whisky Glacier and Davies Dome on James Ross Island (JRI). The mass-balance records of these small glaciers are based on different interpolation methods and volume–mass conversion factors (Table 1). We recalculated surface mass balance (SMB) records (Engel *et al.* 2018) of the two glaciers on JRI using the most widely adopted conversion method in order to assess the impact of different conversion factors and to obtain data that could be directly compared with other records.

Island	Glacier	Latitude	Altitude (m a.s.l.)	Area (km ²)	Snow density (kg·m ⁻³)		Reference
					Accumulation zone	Ablation zone	
King George	Bellingshausen Dome	62°9'S	0–243	12.0	700		Rückamp <i>et al.</i> 2011
					DSP		Mavlyudov 2016
Livingston	Johnsons	62°40'S	0–370	5.4	DSP	900	Navarro <i>et al.</i> 2013
	Hurd	62°41'S	10–370	4.0	DSP	900	
Vega	Bahía del Diablo	63°49'S	0–630	12.9	850 ± 50		Marinsek and Ermolin 2015
James Ross	Davies Dome	63°53'S	0–514	6.5	500 ± 90	900	Engel <i>et al.</i> 2018
	Whisky	63°56'S	215–520	2.4	500 ± 90	900	

Table 1. Snow density values used for volume to mass change conversion in the north-eastern Antarctic Peninsula region. DSP – values determined from density measurements in snow profiles.

Study Area

The investigated glaciers are located in the northern part of JRI (Fig. 1) on the eastern side of the AP. The climate of this region is influenced by the 1000–1800 m

high orographic barrier of the Trinity Peninsula (King *et al.* 2003) and the Southern Annular Mode (Marshall *et al.* 2006). A positive phase in this annular mode increases

north-westerly air flow over the AP and amplifies warming on the eastern side of the AP due to the *foehn* effect (Grosvenor et al. 2014). The warming on the eastern side of the AP has been largest during the summer and autumn months, with the temperatures at Esperanza increasing by $+0.44^{\circ}\text{C}$ per decade over 1952–2015 (Oliva et al. 2017). The mean annual air temperatures (2006–2015) in the northern ice-free part of JRI range from -7.0°C at the sea level (J.G. Mendel station, 10 m a.s.l.) to less than -8.0°C (Bibby Hill, 375 m a.s.l.) in higher-elevation areas (Ambrožová et al. 2019). More frequent positive air

temperatures over the short summer season (two to three months) cause snow and ice to melt on glaciers with large variability depending on cloudiness and solar radiation. The modelled annual precipitation is estimated between 200 and 500 mm water equivalent (van Lipzig et al. 2004). Most of the precipitation falls in solid form and occasional rainfall events are restricted to summer. The distribution of snow cover is strongly influenced by the prevailing south to south-westerly winds, which effectively drift snow from flat relief and ice caps to lee-side surfaces (Kňázková et al. 2019).

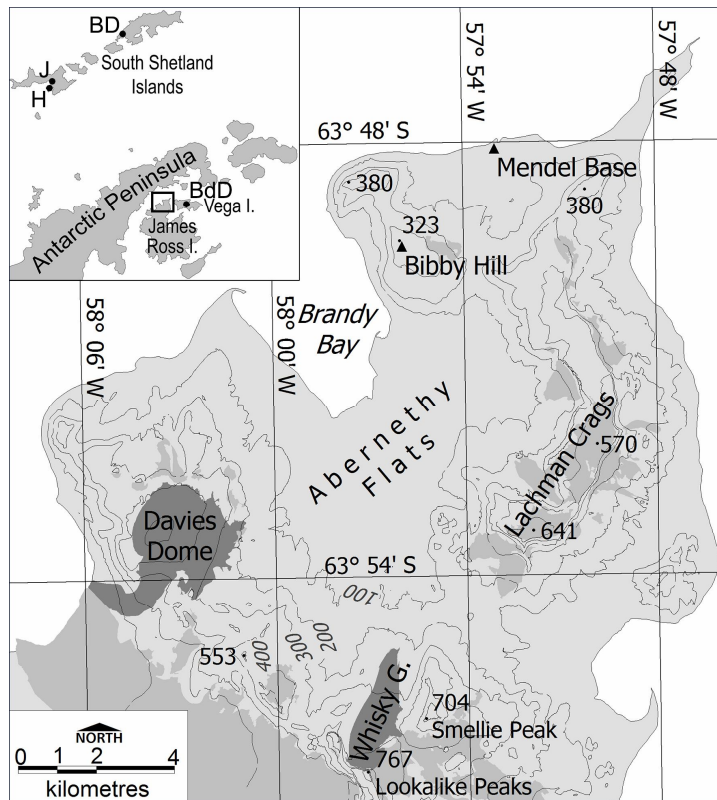


Fig. 1. Location of Davies Dome and Whisky Glacier on the Ulu Peninsula, northern James Ross Island. Other ice bodies are shown in medium grey. Inset shows location of islands and glaciers discussed in this paper: Bellingshausen Dome (BD), Johnsons (J), Hurd (H) and Bahía del Diablo (BdD) glaciers.

The surface of JRI is dominated by a variety of glaciers including the large Mount Haddington Ice Cap (587 km²; Rabassa *et al.* 1982) in the central and southern parts of the island. Bedrock appears at the surface at the periphery of this ice cap and particularly along the northern coast of the island. The largest ice-free area (~180 km²) appears in the northern part of the Ulu Peninsula where glaciers cover only 10% of the land (Fig. 1). Small ice caps and land-terminating valley glaciers are the most frequent glacier systems in this area (Rabassa *et al.* 1982). Because of their small volume, these glaciers are expected to have a relatively fast dynamic response to climatic fluctuations and their mass balance is also considered to be a sensitive indicator of climate change (*e.g.* Allen *et al.* 2008). Therefore, land-terminating valley glacier (Whisky Glacier, *cf.* Chinn and Dillon 1987) and a small ice cap (Davies Dome) were selected for annual mass-balance measurements.

Whisky Glacier (Fig. 2B) is a land-terminating valley glacier (63°55'–63°57'S, 57°56'–57°58'W) located between 520 and 215 m a.s.l. The glacier forms at the foot of ~300 m high north-east face of Lookalike Peaks (767 m a.s.l.), which restricts snow drift on the lee-side surfaces allowing enhanced snow accumulation on the

glacier. An extensive area of debris-covered ice surrounds the western and terminal parts of the glacier while steep western slope of Smellie Peak (704 m a.s.l.) bounds its eastern side. The 3.2 km long glacier is gently inclined (the mean slope of 4°) to the NNE. The mean annual near-surface air temperature in the central part of the glacier is –7.6°C according to the meteorological data collected over the period 2013–2016 (Ambrožová *et al.* 2019).

Davies Dome (Fig. 2A) is an ice dome (63°52'–63°54'S, 58°1'–58°6'W) located ~7 km to the north-west of Whisky Glacier. The dome originates on a volcanic plateau with an elevation of 400–450 m a.s.l. The dome with a flat top at 514 m a.s.l. is elongated in the SW-NE direction being 2.3 km long. The western and northern peripheries of the dome terminate on the plateau whereas the eastern and southern parts descend below the flat surface of the plateau. Most of the eastern margin can be found at an elevation of 210–270 m a.s.l. and only the easternmost tip descends to 170 m a.s.l. The southern part of the dome is drained into Whisky Bay where its 0.7 km wide outlet joins a much wider tidewater glacier forming a 3.3 km long ice cliff. The mean annual near-surface air temperature on the summit of the dome is –8.5°C (Ambrožová *et al.* 2019).

Methods

Surface mass balance determination

Length changes of ablation stakes above the glacier surface recorded annually since 2008/09 with respect to the previous summer values were converted to metres water-equivalent (m w.e.) using (i) the constant density of 850 kg·m⁻³ and (ii) zonally-variable approach (Huss 2013). The second approach reflects variable density of the melted glacier ice in the ablation zone

and snow that persists over a year in the accumulation zone. As snow cover was without superimposed ice, we converted the values in the accumulation and ablation zones using a density of 500 kg·m⁻³ and 900 kg·m⁻³, respectively (Engel *et al.* 2018). Point SMB data were extrapolated over the entire glacier area, allowing the calculation of annual SMB grids.



Fig. 2. Davies Dome (A) and Whisky Glacier (B) as seen from Lachman Crags and Lookalike Peaks, respectively.

As the spatial extrapolation of point data over large areas represents a considerable source of the SMB uncertainty (Huss et al. 2009), we applied the natural neighbour technique that yields the lowest values of the standard and median absolute deviations of the cross validation residuals among the tested interpolation algorithms (Engel et al. 2018). Mass-balance years used in this paper refer to a fixed-date system, with the mass-balance year starting and terminating at the end of austral summer (February). Equilibrium line altitude

(ELA) and accumulation-area ratio (AAR) were determined from the annual mass-balance grids and the surface elevation data. The average elevation of lines with annual zero SMB change is taken from a digital elevation model based on aerial photographs taken in 2006 ([1] - Czech Geological Survey 2009). The accumulation area of the glaciers is determined from the annual mass-balance grids, and divided by the total glacier area to provide annual values of AAR.

Error estimation

The uncertainty in the determination of the annual SMB was estimated following an approach proposed by Huss *et al.* (2009). According to this approach, the uncertainty in the glaciological method arises due to local effects and spatial interpolation:

$$\sigma = \sqrt{\sigma_{local}^2 + \sigma_{int}^2} \quad \text{Eqn. 1}$$

Local uncertainty (σ_{local}) includes uncertainties in the SMB determination at the individual stakes (*e.g.* melt in/out of the stake, reading errors), local variations of snow density (*e.g.* compaction of the snow, percolation and refreezing of meltwater) and thickness changes due to snowdrift (Müller and Kappenberger 1991). As the individual sources of uncertainty in the stake measurements and snowdrift-related thickness changes can be hardly detected, we addressed the estimate of σ_{local} using a simplified approach. In case of the constant density conversion, we assigned an uncertainty of $\pm 60 \text{ kg}\cdot\text{m}^{-3}$ to the ice density for the whole glacier (Huss *et al.* 2009).

For the zonally-variable conversion, we assigned a broad range of uncertainty to the snowpack density for the accumulation area ($\pm 90 \text{ kg}\cdot\text{m}^{-3}$), which should provide a sufficient interval to represent the possible magnitude of the individual sources of uncertainty (Engel *et al.* 2018). The uncertainty that results from spatial interpolation (σ_{int}) is associated with a non-representative distribution of the stakes over the glacier surface, insufficient spatial density of the stakes and the extrapolation of the stake values to unmeasured areas (Huss *et al.* 2009). We estimated this component by the standard deviation of the cross-validation residuals obtained from the interpolation of the annual SMB grids. The determined uncertainty in annual SMB should be considered a lower bound because local variations in the snow thickness are not addressed. The uncertainty in cumulative SMB is calculated as the standard deviation for the period 2009–2015 using the root-sum-square method (Rye *et al.* 2012). Mean values of SMB, ELA and AAR, for this period are reported with the standard error of the mean.

Results

Surface mass-balance changes

SMB of investigated glaciers was calculated based on two different conversion factors as summarised in Table 2. The data indicate higher SMB values determined by the zonally variable conversion factor. A consistent increase of annual values ranges from 0.02–0.08 m w.e. for years with negative SMB to 0.04–0.18 m w.e. for positive years. An increase in cumulative SMB values is higher for Whisky Glacier where higher mass gain was observed over the period 2009–2015. The difference between the cumulative values calculated using the constant and zonally variable conversion

factors attains 0.66 m w.e. for this glacier, while much smaller difference of 0.35 m w.e. was obtained for Davies Dome, where lower surface mass gain was recorded over the same period. The difference between the values calculated by the two approaches is well within the uncertainty range determined for both the annual and cumulative SMB.

The spatial distribution of the annual and cumulative SMB on glaciers reveals similar pattern irrespective of the applied conversion approach (Fig. 3).

Mass-balance year	Whisky Glacier						Davies Dome					
	Constant conversion factor			Zonally variable conversion factor			Constant conversion factor			Zonally variable conversion factor		
	Surface mass balance (m w.e.)	ELA (m)	AAR	Surface mass balance (m w.e.)	ELA (m)	AAR	Surface mass balance (m w.e.)	ELA (m)	AAR	Surface mass balance (m w.e.)	ELA (m)	AAR
2009/10	0.12 ± 0.15	314	0.70	0.06 ± 0.15	316	0.70	0.32 ± 0.21	325	0.70	0.19 ± 0.15	323	0.70
2010/11	0.24 ± 0.06	245	0.96	0.15 ± 0.11	241	0.96	0.12 ± 0.15	377	0.53	0.08 ± 0.12	382	0.59
2011/12	-0.08 ± 0.10	376	0.24	-0.16 ± 0.39	378	0.23	-0.19 ± 0.11	460	0.09	-0.21 ± 0.17	464	0.08
2012/13	0.41 ± 0.22	315	0.79	0.23 ± 0.32	314	0.77	0.20 ± 0.24	367	0.54	0.11 ± 0.20	368	0.53
2013/14	0.13 ± 0.12	320	0.69	0.05 ± 0.25	316	0.68	0.08 ± 0.10	394	0.50	0.04 ± 0.10	395	0.49
2014/15	0.41 ± 0.42	299	0.74	0.23 ± 0.32	301	0.73	-0.07 ± 0.08	420	0.21	-0.09 ± 0.13	423	0.23
Mean 2009–2015	0.21 ± 0.07	312 ± 16	0.69 ± 0.09	0.09 ± 0.05	311 ± 16	0.68 ± 0.09	0.08 ± 0.07	391 ± 17	0.43 ± 0.09	0.02 ± 0.05	393 ± 18	0.44 ± 0.09
Cumulative 2009–2015	1.23 ± 0.44			0.57 ± 0.67			0.46 ± 0.36			0.11 ± 0.37		

Table 2. Surface mass balance characteristics for Whisky Glacier and Davies Dome calculated using constant and zonally variable conversion factors over the period 2009–2015.

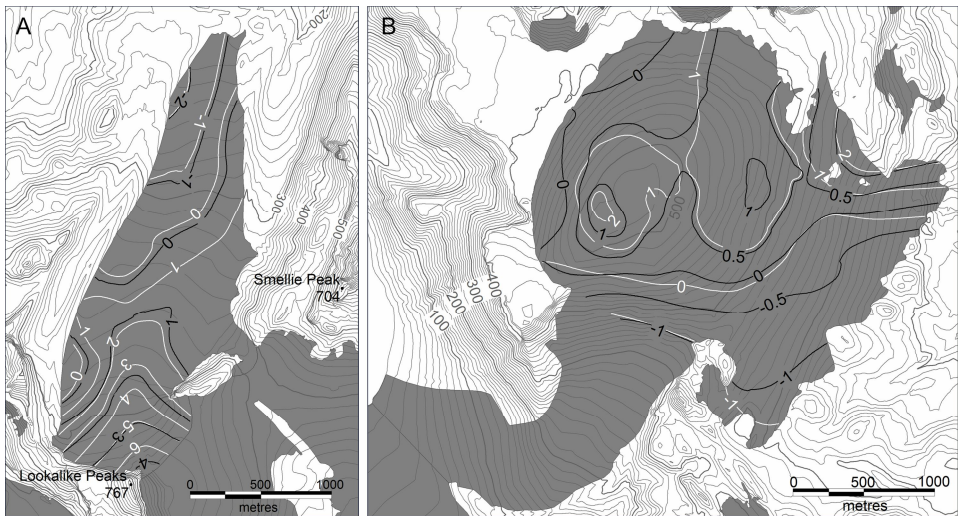


Fig. 3. Cumulative surface mass balance (in m w.e.) on Whisky Glacier (A) and Davies Dome (B) over the period 2009–2015. Black and white lines indicate surface mass balance values determined using zonally-variable approach and constant density, respectively.

The pattern is almost identical in the ablation zone where conversion factors of 850 and 900 $\text{kg}\cdot\text{m}^{-3}$ yield very similar SMB values. Isolines that represent spatial distribution of the SMB are also nearly parallel in the accumulation zone of Whisky Glacier but values obtained by the constant conversion factor progressively increase towards higher elevation (Fig. 3A). The simi-

larity in pattern above the ELA is less clear on Davies Dome where application of the density of 500 $\text{kg}\cdot\text{m}^{-3}$ for snow results in limited mass gain (Fig. 3B). The constant conversion factor results in larger range of SMB values that applies to cumulative and most of annual values determined for the investigated glaciers over the period 2009–2015.

Equilibrium line altitude and accumulation-area ratio

The mean ELA for Whisky Glacier over the period 2009–2015 was determined to be 312 ± 16 m and 311 ± 16 m using the constant and zonally-variable conversion factors, respectively. For Davies Dome, the zonally-variable approach yields mean ELA of 393 ± 18 m that is by 2 m higher than the value obtained by the constant conversion factor. The annual ELAs differ by up to 4 m for Whisky Glacier and 1 to 5 m for Davies Dome (Table 2). However, equilibrium lines obtained by the two approaches for individual years and for the investigated period are nearly parallel (Fig. 3). The equilibrium lines determined by the zonally-variable approach are located mostly within a narrow 5 to 10-m elevation zone below the lines derived by the constant conversion factor. The higher elevation difference between the equilibrium lines on Davies Dome (Fig. 3B) is in accordance

with more complex layout and surface topography of this glacier (Engel *et al.* 2018).

The two applied conversion factors yield similar AAR values. Mean AAR values determined for Whisky Glacier over the period 2009–2015 using the constant and zonally-variable conversion factors are 0.69 ± 0.09 and 0.68 ± 0.09 , respectively. The same difference between the AAR values was obtained for Davies Dome, where the zonally-variable approach yields mean AAR of 0.44 ± 0.09 . The difference between annual AAR values determined by the two conversion approaches ranges is small ranging mostly from 0 to 0.02 on both glaciers (Table 2). A higher difference was obtained only for the mass-balance year 2010/11, for which constant conversion approach yields by 0.06 higher AAR value on Davies Dome compared to the zonally-variable conversion.

Discussion

The comparison of SMB values determined for Whisky Glacier and Davies Dome over the period 2009–2015 with the SMB records from the northern AP region suggests that the zonally-variable conversion factor gives more realistic results. The data calculated using the zonally-variable conversion factor better fits to cumulative values of surface mass changes reported from glaciers in this region (Fig. 4). Lower SMB values obtained for investigated gla-

ciers based on this conversion are in accordance with the location of JRI at the leeward precipitation shadow of AP, where the modelled precipitation ranges from 200 to 500 mm w.e. (van Lipzig *et al.* 2004) and the mean annual air temperature is 4 to 7°C lower compared to SSI (Ambrožová *et al.* 2019, Oliva *et al.* 2017). By contrast, glaciers on SSI receive more precipitation (500 to 1000 mm w.e.) that is considered to represent the most important SMB com-

ponent over the AP (van Lipzig et al. 2004). The results of the zonally-variable approach are in agreement with the SMB data reported from the Bahía del Diablo Glacier (Marinsek and Ermolin 2015), which represents the same part of the AP

with similar climate conditions to northern JRI. The application of constant conversion factor over the investigated glacier surface overestimates mass gain yielding 50 to 150% higher SMB values that are probably unrealistic.

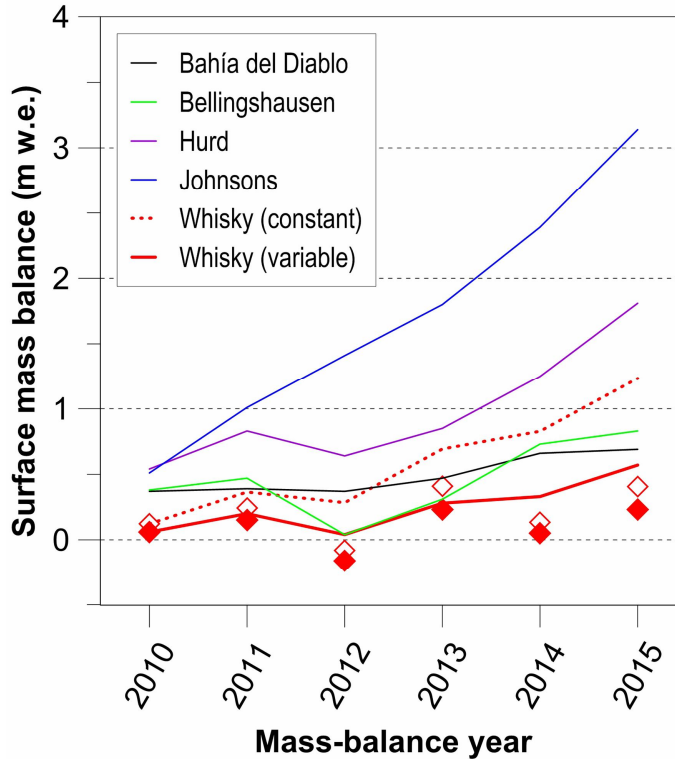


Fig. 4. Cumulative values of surface mass-balance changes (relative to summer 2008/09) of glaciers around the northern Antarctic Peninsula over the period 2009–2015. Black thick and thin lines indicate surface mass balance of Whisky Glacier determined using zonally-variable approach and constant density, respectively. Solid (zonally-variable density) and unfilled (constant density) diamonds show annual surface mass values of this glacier. Data adopted from Mavlyudov (2016), WGMS (2017) - [2], Engel et al. (2018).

The applied conversion factor does not affect ELA and AAR values. These characteristics determined for Whisky Glacier and Davies Dome are in agreement with the data reported for Bahía del Diablo Glacier (*see* [2] - WGMS 2017). The temporal changes in ELA coincide over that period except for 2009/10 when Bahía del Diablo

Glacier experienced the largest mass gain since 2000 and its ELA was located much lower than on the investigated glaciers on JRI (Engel et al. 2018). The ELA values determined for the investigated glaciers are significantly higher compared with the glaciers on SSI and the trend of ELA changes started to differ from glaciers on

SSI after 2012/13. While ELA experienced a decrease on SSI, it increased on the investigated glaciers and Bahía del Diablo Glacier. The observed difference in ELA may indicate lower precipitation and colder conditions on JRI and Vega Island (van Lipzig *et al.* 2004, Oliva *et al.* 2017). The previous studies show that the SSI glaciers are very sensitive to air temperatures (Blindow *et al.* 2010, Jonsell *et al.* 2012) and the

associated changes in large-scale circulation pattern (Braun *et al.* 2001). The reported stronger sensitivity is also related to the fact that average summer temperatures on these glaciers often fluctuate around zero, and therefore even a small temperature change may cause a rapid shift from melting to freezing conditions and *vice versa* (Breuer *et al.* 2006).

Concluding remarks

The comparison of SMB data determined using the constant and zonally-variable conversion factor reveals that zonally-variable approach provides lower annual and cumulative SMB values. The difference between the cumulative values calculated using the density of $850 \text{ kg}\cdot\text{m}^{-3}$ for the whole glacier and ice/snow density of $500/900 \text{ kg}\cdot\text{m}^{-3}$ for ablation/accumulation zones is higher for Whisky Glacier ($1.23 \pm 0.44/0.57 \pm 0.67 \text{ m w.e.}$) where a total mass gain was observed over the period 2009–2015. The variation of annual and cumulative ($0.46 \pm 0.36/0.11 \pm 0.37 \text{ m w.e.}$) SMB values is lower for Davies Dome, where lower surface mass gain was recorded over the same period. The difference between the values calculated by the two approaches is well within the uncertainty range determined for both the annual and cumulative SMB.

The comparison of SMB values obtained from the two conversion approaches with SMB data from the northern AP region suggests that zonally-variable conversion factor provides more accurate data. The results suggest that this approach yields SMB values that better fit to the range of SMB records from SSI (Bellingshausen Ice Dome, Hurd and Johnsons glaciers) and Vega Island (Bahía del Diablo Glacier) and is thus advisable.

The determined mass balance changes suggest that the conversion approach does

not affect much the spatial distribution of the annual and cumulative SMB on glaciers. The annual pattern of the SMB is almost identical in the ablation zone and very similar in the accumulation zone. The constant conversion factor yields higher SMB values above equilibrium line showing the spatial distribution of the SMB in larger detail. The same applies to the cumulative SMB distribution over the period 2009–2015.

The variation of determined ELA and AAR values is low irrespective of the conversion approach. The data indicates that if the constant conversion factor is used the annual ELA and AAR differ from the values obtained by the zonally-variable approach by less than 5 m and 0.06, respectively. Thus, concerns about the negative influence of constant conversion factor on ELA and AAR do not apply.

The observed annual changes of ELA and the mean ELAs determined for Whisky Glacier ($311 \pm 16 \text{ m a.s.l.}$) and Davies Dome ($393 \pm 18 \text{ m a.s.l.}$) over the period 2009–2015 coincide with the values reported from Bahía del Diablo Glacier but differ from the glaciological records on SSI. The opposite trend of ELA values determined for glaciers at the eastern side of AP and SSI after 2012/13 confirms that different climate factors control the annual changes in glacier mass in these two regions.

References

- ALLEN, R. J., SIEGERT, M. J. and PAYNE, T. (2008): Reconstructing glacier-based climates of LGM Europe and Russia – Part 1: Numerical modelling and validation methods. *Climate of the Past*, 4: 235-248.
- AMBROŽOVÁ, K., LÁSKA, K., HRBÁČEK, F., KAVAN, J. and ONDRUCH, J. (2019): Air temperature variability and altitudinal dependence in the ice-free and glaciated areas of northern James Ross Island, Antarctic Peninsula. *International Journal of Climatology*, 39: 643-657.
- BLINDOW, N., SUCKRO, S. K., RÜCKAMP, M., BRAUN, M., SCHINDLER, M., BREUER, B., SAUBER, H., SIMÕES, J. C. and LANGE, M. A. (2010): Geometry and thermal regime of the King George Island ice cap, Antarctica, from GPR and GPS. *Annals of Glaciology*, 51: 103-109.
- BRAUN, M., SAURER, H., VOGT, S., SIMÕES, J. and GOSSMAN, H. (2001): The influence of large-scale atmospheric circulation on the surface energy balance of the King George Island ice cap. *International Journal of Climatology*, 21: 21-36.
- BREUER, B., LANGE, M. and BLINDOW, N. (2006): Sensitivity studies on model modifications to assess the dynamics of a temperate ice cap, such as that on King George Island, Antarctica. *Journal of Glaciology*, 52: 235-247.
- CHINN, T. J. H., DILLON, A. (1987): Observations on a debris-covered polar glacier ‘Whisky Glacier’, James Ross Island, Antarctic Peninsula, Antarctica. *Journal of Glaciology*, 33: 300-310.
- ENGEL, Z., LÁSKA, K., NÝVLT, D. and STACHOŇ, Z. (2018): Surface mass balance of small glaciers on James Ross Island, north-eastern Antarctic Peninsula, during 2009–2015. *Journal of Glaciology*, 64: 349-361.
- GROSVENOR, D. P., KING, J. C., CHOULARTON, T. W. and LACHLAN-COPE, T. (2014): Downslope föhn winds over the Antarctic Peninsula and their effect on the Larsen ice shelves. *Atmospheric Chemistry and Physics*, 14: 9481-9509.
- HUSS, M. (2013): Density assumptions for converting geodetic glacier volume change to mass change. *The Cryosphere*, 7: 877-887.
- HUSS, M., BAUDER, A. and FUNK, M. (2009): Homogenization of longterm mass-balance time series. *Annals of Glaciology*, 50: 198-206.
- JONSELL, U. Y., NAVARRO, F. J., BAÑÓN, M., LAPAZARAN, J. J. and OTERO, J. (2012): Sensitivity of a distributed temperature-radiation index melt model based on AWS observations and surface energy balance fluxes, Hurd Peninsula glaciers, Livingston Island, Antarctica. *The Cryosphere*, 6: 539-552.
- KING, J. C., TURNER, J., MARSHALL, G. J., CONNOLLEY, W. M. and LACHLAN-COPE, T. A. (2003): Antarctic Peninsula climate variability and its causes as revealed by instrumental records. In: E. Domack, A. Leventer, A. Burnett, R. Bindshadler, P. Convey and M. Kirby (eds.): *Antarctic Peninsula Climate Variability: Historical and Paleoenvironmental Perspectives*, American Geophysical Union, Washington, pp. 17–30.
- KŇAŽKOVÁ, M., HRBÁČEK, F., NÝVLT, D. and KAVAN, J. (2019, *in press*): Effect of hyaloclastite breccia boulders on meso-scale periglacial-aeolian landsystem in semi-arid Antarctic environment, James Ross Island, Antarctic Peninsula. *Cuadernos de Investigacion Geografica*.
- MARINSEK, S., ERMOLIN, E. (2015): 10 year mass balance by glaciological and geodetic methods of Glacier Bahía del Diablo, Vega Island, Antarctic Peninsula. *Annals of Glaciology*, 56: 141-145.
- MARSHALL, G. J., ORR, A., VAN LIPZIG, N. and KING, J. C. (2006): The impact of a changing Southern Hemisphere Annular Mode on Antarctic Peninsula summer temperatures. *Journal of Climate*, 19: 5388-5404.
- MAVLYUDOV, B. R. (2016): Bellingshausen Ice Dome, Antarctic. In: V. M. Kotlyakov (ed.): *Problems of geography, Geography of Polar Regions*, v. 142, Codex, Moscow, pp. 629–648. (In Russian).
- MÜLLER, H., KAPPENBERGER, G. (1991): Claridenfirn-Messungen 1914–1984. *Zürcher Geografische Schriften*, 40.

- NAVARRO, F. J., JONSELL, U. Y., CORCUERA, M. I. and MARTÍN-ESPAÑOL, A. (2013): Decelerated mass loss of Hurd and Johnsons Glaciers, Livingston Island, Antarctic Peninsula. *Journal of Glaciology*, 59: 115-128.
- OLIVA, M., NAVARRO, F., HRBÁČEK, F., HERNANDEZ, A., NÝVLT, D., PERREIRA, P., RUIZ-FERNADÉZ, J. and TRIGO, R. (2017): Recent regional climate cooling on the Antarctic Peninsula and associated impacts on the cryosphere. *Science of the Total Environment*, 580: 210-223.
- PFEFFER, W. T., ARENDT, A. A., BLISS, A., BOLCH, T., COGLEY, J. G., GARDNER, A. S., HAGEN, J. O., HOCK, R., KASER, G., KIENHOLZ, C., MILES, E. S., MOHOLDT, G., MOLG, N., PAUL, F., RADIC, V., RASTNER, P., RAUP, B., RICH, J. and SHARP, M. (2014): The Randolph Glacier Inventory: a globally complete inventory of glaciers. *Journal of Glaciology*, 60: 537-552.
- RABASSA, J., SKVARCA, P., BERTANI, L. and MAZZONI, E. (1982): Glacier inventory of James Ross and Vega Islands, Antarctic Peninsula. *Annals of Glaciology*, 3: 260-264.
- RÜCKAMP, M., BRAUN, M., SUCKRO, S. and BLINDOW, N. (2011): Observed glacial changes on the King George Island ice cap, Antarctica, in the last decade. *Global and Planetary Change*, 79: 99-109.
- RYE, C. J., WILLIS, I. C., ARNOLD, N. S. and KOHLER, J. (2012): On the need for automated multiobjective optimization and uncertainty estimation of glacier mass balance models. *Journal of Geophysical Research*, 117: F02005.
- VAN LIPZIG, N. P. M., KING, J. C., LACHLAN-COPE, T. A. and VAN DEN BROEKE, M. R. (2004): Precipitation, sublimation, and snow drift in the Antarctic Peninsula region from a regional atmospheric model. *Journal of Geophysical Research*, 109: D24106.

Web sources / Other sources

- [1] Czech Geological Survey (2009) James Ross Island – Northern Part. Topographic map 1 : 25 000. CGS, Praha.
- [2] WGMS (2017): *Fluctuations of Glaciers Database*. World Glacier Monitoring Service, Zürich (doi: 10.5904/wgms-fog-2017-06).